Snow Melt Onset Over Arctic Sea Ice from SMMR and SSM/I-SSMIS Brightness Temperatures, Version 4

USER GUIDE

How to Cite These Data

As a condition of using these data, you must include a citation:

Anderson, M., A. C. Bliss, and S. Drobot. 2019. *Snow Melt Onset Over Arctic Sea Ice from SMMR and SSM/I-SSMIS Brightness Temperatures, Version 4.* [Indicate subset used]. Boulder, Colorado USA. NASA National Snow and Ice Data Center Distributed Active Archive Center. https://doi.org/10.5067/A9YK15H5EBHK. [Date Accessed].

FOR QUESTIONS ABOUT THESE DATA, CONTACT NSIDC@NSIDC.ORG

FOR CURRENT INFORMATION, VISIT https://nsidc.org/data/NSIDC-0105

National Snow and Ice Data Center

TABLE OF CONTENTS

1 DATA DESCRIPTION

1.1 Parameters

The main parameter for this data set is the Snow Melt Onset Date (SMOD) over Arctic sea ice, or the Day of Year (DOY) when microwave brightness temperatures increase sharply due to the presence of liquid water in the snowpack. This data set also includes statistical analyses of each grid cell's SMOD over the period between 1979 through 2017. Table 1 includes a description of valid SMOD values, while Table 2 contains a description of valid statistical fields.

Table 1.SMOD Values and Descriptions

Value	Description
5	Pole hole; no melt date was calculated
10	Water (ocean, lakes); no melt date was calculated
15	Land; no melt date was calculated
61-245	Day of snow melt onset, recorded as the Day of Year (DOY)
255	Sea ice did not melt; no melt data was calculated

Table 2. Valid Parameter Range for Statistics Fields

Value	Description
-150	No data; open water or missing melt date
-100	Pole hole; no melt dates were calculated
-50	Land mask; no melt dates were calculated
-30 to 255	Valid data

1.2 File Information

1.2.1 Format

Data are provided in netCDF (.nc) file format.

PNG (.png) browse images and Extensible Markup Language (.xml) files with associated metadata are also provided.

1.2.2 File Contents

NetCDF file contents are described in Table 3.

Table 3.Description of netCDF Variables

Variable Name	Description	Units
SMOD	Annual snow melt onset date	Day of Year (DOY); see Table 1 for more details
mean	Mean snow melt onset date	DOY
median	Median snow melt onset date	DOY
latest	Latest (maximum) snow melt onset date	DOY
earliest	Earliest (minimum) snow melt onset date	DOY
range	Latest minus earliest snow melt onset date	Days
stdev	Standard deviation of snow melt onset dates	Days
trend	Decadal trend in snow melt onset based on a least squares linear regression	Days per Decade
latitude	Latitude	Degrees North
longitude	Longitude	Degrees East
projection	Description of projected coordinate system	N/A
time	Time	Days since 1970-01-01
x	Projected x coordinate	Meters
y	Projected y coordinate	Meters

One browse image is provided for each year of data showing the annual SMOD; Figure 1 contains a sample image. One browse image is also provided for each statistical field, as exemplified by Figure 2.

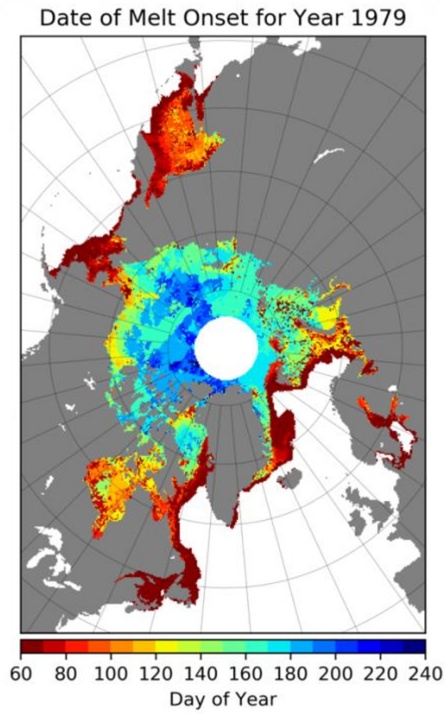

Figure 1. Sample browse image showing snow melt onset dates for 1979.

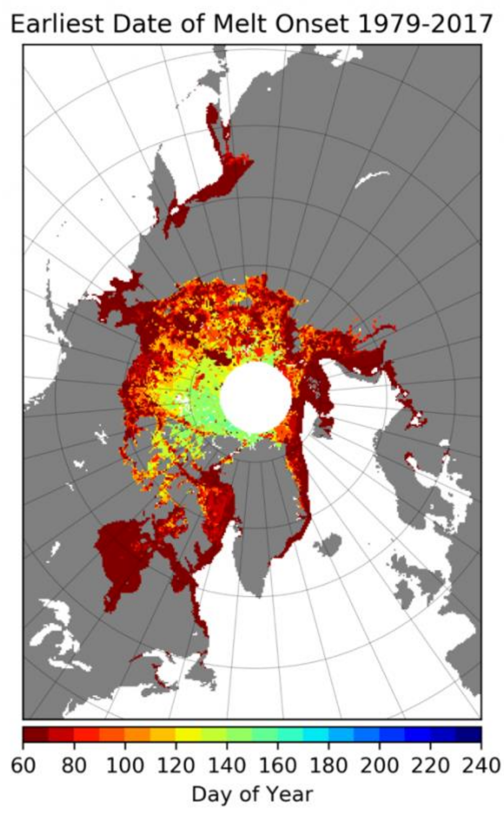

Figure 2. Sample statistical-field browse image showing

the earliest snowmelt onset date recorded between 1979 and 2017.

1.2.3 Directory Structure

Data are available for download via HTTPS; the link is accessible through the "Download Data" tab on the data set landing page. Within the file directory, browse images are available in the subfolder labeled "Browse."

1.2.4 Naming Convention

The netCDF file name is:

```
SMOD_1979-2017_v04r00.nc
```

Browse images showing the annual snow melt onset date are named according to the following convention and as described in Table 4:

```
melt_<year>_v04r00_n.png
```

Table 4. Snow Melt Onset Date Browse Images

Variable	Description
melt	Indicates the file is part of the Snow Melt Onset Over Arctic Sea Ice from SMMR and SSM/I-SSMIS Brightness Temperatures data set
<year>	Year of data represented by the image
v04	Data set version number (e.g. 04)
r00	Data set revision number (e.g. 00)
n	Hemisphere (n = Northern)

Browse images for statistical fields are named according to the following convention and as described in Table 5:

```
melt_<field>_1979-2017_v04r00.png
```

Table 5. Statistical Browse Images

Variable	Description
melt	Indicates the file is part of the Snow Melt Onset Over Arctic Sea Ice from SMMR and SSM/I-SSMIS Brightness Temperatures data set
<field>	Statistical field represented in the image (e.g. range, earliest, latest)
1979-2017	Data set temporal coverage
v04	Data set version number (e.g. 04)
r00	Data set revision number (e.g. 00)

1.2.5 File Size

The netCDF file is approximately 1.9 MB.

Browse images are approximately 345 KB.

1.3 Spatial Information

1.3.1 Coverage

Data cover the Northern Hemisphere, except for three circular gaps centered over the pole that correspond to the three satellite records. Data from the SMMR period (1978-87) have a gap with a radius of 611 km, located poleward of 84.5 degrees North. Data from the SSM/I period (1987 through 2007) have a polar gap with a radius of 311 km, located poleward of 87.2 degrees North. Lastly, data from the SSMIS period (2008 through 2017) have a gap poleward of 89.2° North. See the Polar Stereographic Projection and Grid spatial coverage map for details.

1.3.2 Resolution

25 km

1.3.3 Geolocation

The data are provided on the 25 km Northern Hemisphere Polar Stereographic Grids, as described in Tables 6 and 7. For more information, see the Polar Stereographic Projections and Grid web page.

Table 6. Geolocation Details

Geographic coordinate system	Unspecified datum based upon the Hughes 1980 ellipsoid
Projected coordinate system	NSIDC Sea Ice Polar Stereographic North
Longitude of true origin	-45
Latitude of true origin	70
Scale factor at longitude of true origin	1
Datum	Not_specified_based_on_Hughes_1980_ellipsoid
Ellipsoid/spheroid	Hughes 1980
Units	meter
False easting	0
False northing	0
EPSG code	3411
PROJ4 string	+proj=stere +lat_0=90 +lat_ts=70 +lon_0=-45 +k=1 +x_0=0 +y_0=0 +a=6378273 +b=6356889.449 +units=m +no_defs
Reference	https://epsg.io/3411

Table 7. Grid Details

Grid cell size (x, y pixel dimensions)	25.0 km
Number of rows	448
Number of columns	304
Geolocated lower left point in grid	33.92° N, 279.26° W
Nominal gridded resolution	25 km x 25 km
Grid rotation	N/A
ulxmap – x-axis map coordinate of the center of the upper-left pixel (XLLCORNER for ASCII data)	-3850 projected km
ulymap – y-axis map coordinate of the center of the upper-left pixel (YLLCORNER for ASCII data)	5850 projected km

1.4 Temporal Information

1.4.1 Coverage

his data set extends from 1979 through 2017. Snow melt onset dates were derived from brightness temperatures acquired from multiple platforms, as described in Table 8. For all years, only brightness temperatures from DOY 61 (early March) through 245 (early September) were used to calculate snow melt onset dates.

Table 8. Temporal Coverage by Input Sensor

Platform / Sensor	**Start Date**	**End Date**
Nimbus-7 SMMR	01 Jan 1979	20 August 1987[1]
DMSP F8 SSM/I	01 Jan 1988	18 December 1991
DMSP F11 SSM/I	01 Jan 1992	31 December 1995
DMSP F13 SSM/I	01 Jan 1996	31 December 2007
DMSP F17 SSMIS	01 Jan 2008	31 December 2017
[1]Other data was not substituted for the missing SMMR data to cover the last 11 days of the melt season in August 1987. Those days are flagged as "no data."		

1.4.2 Resolution

Snow melt onset dates were derived once per year for each grid cell.

2 DATA ACQUISITION AND PROCESSING

2.1 Background

Accurate snow melt onset dates over sea ice contribute to improved simulations of climate during the Arctic snow melt period. Records of the spatial and temporal variability in snow melt can also serve as climate proxies in Arctic sea ice zones.

Snow melt onset dates are estimated based on changes in brightness temperature measurements. Microwave emissivity of snow increases dramatically as the snow melts and liquid water appears. With the presence of liquid water in the snow pack, surface scattering dominates over volume scattering, resulting in a sharp increase in the brightness temperatures signature. Lower microwave frequencies (e.g. 18.0 GHz and 19.3 GHz) are more responsive to melt onset in ice than are higher frequencies (e.g. 37.0 GHz), primarily due to the change in emission depth associated with melt. Melt therefore causes the difference between low-frequency and high-frequency brightness temperatures to change from positive to near-zero or negative. Furthermore, the increase in brightness temperature associated with melt is polarization-dependent. Horizontal channels reflect a stronger dependence on snow conditions during melt due to the change in dielectric properties at the air-snow interface when snow is wet.

2.2 Acquisition

Snow melt onset dates were derived from brightness temperature (Tb) measurements acquired by the Scanning Multichannel Microwave Radiometer (SMMR), Special Sensor Microwave/Imager (SSM/I), and Special Sensor Microwave Imager/Sounder (SSMIS) instruments. Sea ice extent masks were also used to constrain the melt algorithm. Table 9 describes the input data sources in more detail.

Table 9. Input Data Sets

Data Set	Description	Channels/Variables Used
Nimbus-7 SMMR Polar Gridded Radiances and Sea Ice Concentrations, Version 1 (Gloersen 2006)	T_b used to calculate snow melt onset dates from 1979 to 1987.	18.0 GHz and 37.0 GHz
DMSP SSM/I-SSMIS Daily Polar Gridded Brightness Temperatures, Version 4 (Maslanik and Stroeve 2004)	T_b used to calculate snow melt onset dates from 1988 to 2017.	19.3 GHz and 37.0 GHz
NOAA/NSIDC Climate Data Record of Passive Microwave Sea Ice Concentration, Version 3 (Meier et al. 2017)	Sea ice concentrations used to a create mask of the annual sea ice maximum extent. Snow melt dates were only calculated for locations inside the sea ice mask.	goddard_merged_seaice_conc

2.3 Processing

Snow melt onset dates were estimated using daily average brightness temperature (Tb) data from SMMR, SSM/I (F8, F11, and F13), and SSMIS (F17) satellite radiometers. Changes in 18.0 or 19.3 H-polarization GHz and 37.0 H-polarization GHz Tb were recorded for each grid cell using the Advanced Horizontal Range Algorithm (AHRA). For more details on AHRA, please refer to Anderson 1997.

1. **Ensure consistent input data**

For this data set, SSM/I F8 was used as the standard input sensor. Regression analysis was used to convert SMMR, SSM/I F11 and F13, and SSMIS F17 Tb to SSM/I F8 Tb (after Abdalati et al. 1995). Table 10 provides an overview of the correction coefficients used.
These conversions ensure a consistent data record for determining temporal trends in the snow melt onset dates. If data are not consistent, snow melt trends could be attributable to instrument characteristics rather than climate conditions.

2. **Created sea ice extent mask**

The goddard_merged_seaice_conc variable from the NOAA/NSIDC Climate Data Record of Passive Microwave Sea Ice Concentration, Version 3 data set was used as a measure of daily Sea Ice Concentration (SIC). Beginning on Day of Year (DOY) 61 (early March), these SIC estimates were used to determine which pixels had a SIC ≥ 50%. Snow melt onset dates were only calculated at pixel locations that met this criterion.

- DOY 61 was used because this date roughly corresponds to the time period of maximum annual sea ice extent.
- Since the SMMR data were collected every other day, in the event of data outages (i.e. a missing swath), a SIC ≥ 50% for any day between DOY 61 and DOY 65 was used to define the sea ice extent.
- A unique sea ice extent mask was created for each year of data.

3. **Run AHRA**

The AHRA calculates the difference between low-frequency (18.0 GHz or 19.3 GHz) and high-frequency (37.0 GHz) Tb measurements. When conditions are dry and frozen, low-frequency Tb measurements are larger than high-frequency Tb measurements. When low-frequency Tb drop below high-frequency Tb measurements, melt has started. Turn points are described below; refer to Drobot and Anderson 2001 for more details.

- If (18.0 / 19.3 GHz - 37.0 GHz) > 4 K, the AHRA assumes winter conditions and proceeded to the next day with data for that pixel.
- If (18.0 / 19.3 GHz - 37.0 GHz) ≤ -10 K, the AHRA assumes liquid water was present in the snowpack and classifies that day as the snow melt onset date.
- If 4 K > (18.0 / 19.3 GHz - 37.0 GHz) > -10 K, the AHRA determines if snow melt onset occurred based on a 20-day time series of Tb. The algorithm subtracts the minimum and maximum Tb values for the ten days prior to the potential melt onset date, and again for the period from the potential melt onset date to nine days later. The former number is then subtracted from the latter number. If the difference is greater than 7.5 K, the algorithm assigns a snow melt onset date to that particular grid cell because a large difference indicates variability in the 18.0 / 19.3 GHz - 37.0 GHz range after the potential melt onset

date. If the difference was less than 7.5 K, then liquid water is unlikely to be in the snowpack, and the algorithm moves on to the next day.

4. **Assigned quality flags**
   - Assigned a value of 5 to all pixels that were part of the pole hole.
   - Assigned a value of 10 to all pixels that were over open ocean.
   - Assigned a value of 15 to all pixels that were over land.
   - Assigned a value of 255 to all pixels where melt was not calculated.

Table 10. Linear Regression Coefficients and Equations Used to Calibrate TBs Between SMMR, SSMI, and SSMIS Sensors using F8 as the Standard

Sensor Correction	Source	Overlap Area	Channels	Coefficients		Correction Equation
SMMR to F8	Jezek et al. (1991)	---	18H	Slope	0.940	F8=(SMMR-2.62)/0.940
				Int. (K)	2.62	
			37H	Slope	0.954	F8=(SMMR-2.85)/0.954
				Int. (K)	2.85	
F11 to F8	Abdalati et al. (1995)	Greenland	19H	Slope	1.013	F8=1.013*F11-1.890
				Int. (K)	-1.89	
			37H	Slope	1.024	F8=1.024*F11-4.220
				Int. (K)	-4.22	
F13 to F11	Stroeve et al. (1998)	NH Sea Ice	19H	Slope	0.986	F11=(F13-2.197)/0.986
				Int. (K)	2.179	
			37H	Slope	0.966	F11=(F13-6.110)/0.966
				Int. (K)	6.11	
F17 to F13	Meier et al. (2011)	Arctic Mar - Sept 2007	19H	Slope	0.979	F13=(F17-1.646)/0.979
				Int. (K)	1.646	
			37H	Slope	0.999	F13=(F17-0.649)/0.999
				Int. (K)	0.649	

2.4 Quality, Errors, and Limitations

2.4.1 Differences between V3 and V4 Data

The differences between the Version 3 (V3) and Version 4 (V4) snow melt onset dates (SMOD) are illustrated for two years in Figure 3. Differences are limited to the sea ice edge and around the pole hole. Along the ice edge, blue pixels indicate grid cells where SMOD was computed in V4 but not V3. Conversely, red pixels along the ice edge indicate grid cells where SMOD was computed in V3 but not in V4. These differences are due to slight variations in the V2 and V3 NOAA/NSIDC

Climate Data Record of Passive Microwave Sea Ice Concentration data sets, which were used to create the sea ice masks in V3 and V4 of this data set, respectively.

The biggest differences between V3 and V4 SMOD occur at the pole hole in the years 2008 - 2012. In the previous SIC data version, a larger pole hole was used to mask SICs obtained using SSMIS; thus, no SMOD could be computed within this region. However, the updated SIC data now use a smaller pole hole mask for these years, which allows SMOD to be computed. These new SMOD are shown as the dark blue ring in Figure 3 (right panel) surrounding the North Pole. Note that almost differences exist between V3 and V4 SMOD for the bulk of the sea ice area because no changes have bene made to the AHRA algorithm since publication by Bliss and Anderson (2014).

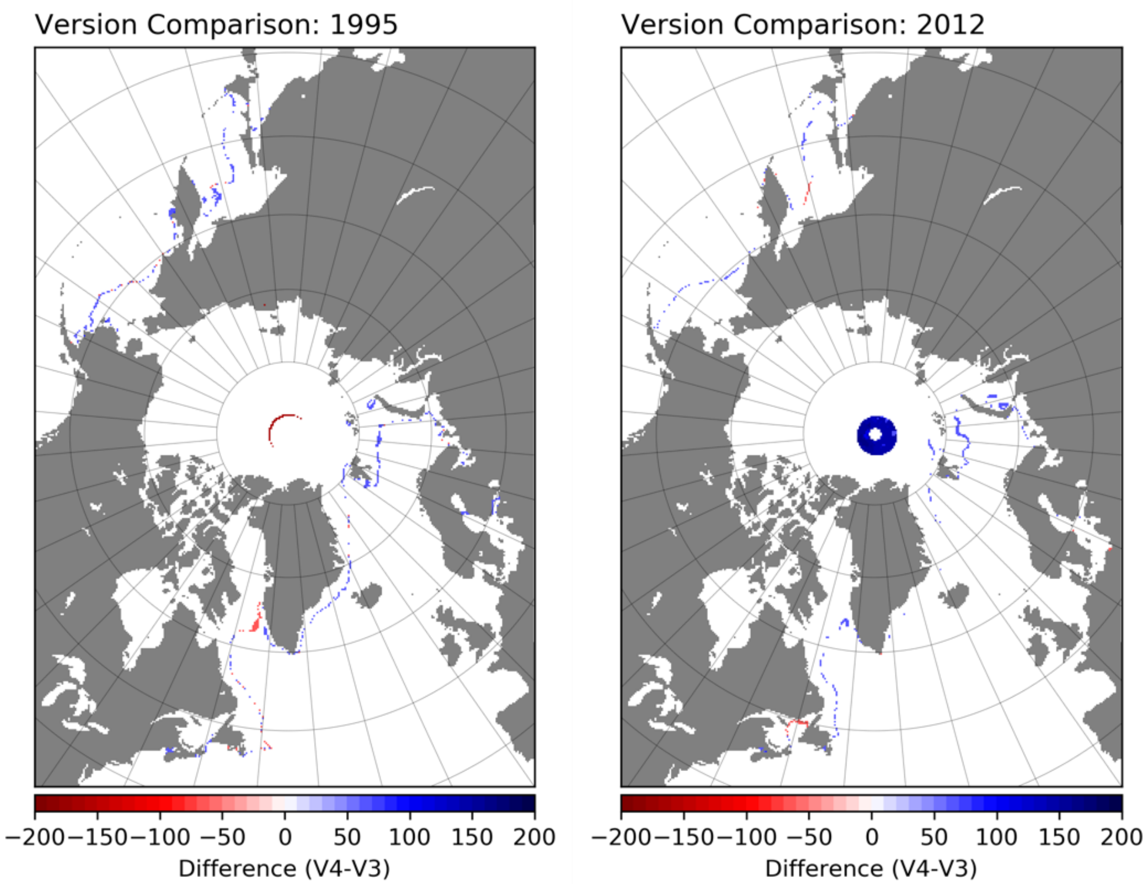

Figure 3. Visual comparison of snow melt onset dates from Version 3 and Version 4 of this data set.

2.4.2 Error Sources

Brightness temperature data may have errors related to pixel averaging, sensor errors, and weather effects. See the following brightness temperature documentation for more information regarding errors in the source data:

- DMSP SSM/I-SSMIS Daily Polar Gridded Brightness Temperatures

- Nimbus-7 SMMR Polar Radiances and Arctic and Antarctic Sea Ice Concentrations

2.4.3 Limitations

Given the known errors, users are advised against selecting individual pixels without examining surrounding data points. Also, trend analysis at any given pixel should include a study of nearby pixels to confirm that results are locally consistent.

2.5 Instrumentation

Brightness temperature input data were acquired from the Scanning Multichannel Microwave Radiometer (SMMR), Special Sensor Microwave/Imager (SSM/I), and Special Sensor Microwave Imager/Sounder (SSMIS) instruments. For more details, refer to the SMMR, SSM/I, and SSMIS Sensors Summary.

3 SOFTWARE AND TOOLS

For a comprehensive list of all polar stereographic tools, see the Polar Stereographic Data Tools Web page.

4 VERSION HISTORY

Table 11 outlines the processing and algorithm history for this product.

Table 11. Description of Version Changes

Version	Date	Description of Changes from Previous Version
V04	June 2019	Reprocessed the entire data set using a newer version of the sea ice extent masks within the snow melt onset algorithm. No other changes were made to the algorithm. Extended the data record through 2017. After snow melt dates were computed, flags were added to the data to indicate where snow melt dates were not derived. The flags discriminate between sea ice where the snow melt onset date was not found and pixels included in the land mask, the pole hole, and areas of open water. Updated data fields that summarize basic statistics over the length of the data record. Data are now distributed as a netCDF file.
V03	Mar 2014	Extended data record through the 2012 melt season which includes the use of the SSMIS instrument on the DMSP F17 satellite. Removed the two-pixel buffer surrounding the coastlines. Included the use of an annual sea ice extent mask to indicate sea ice locations where a melt onset date was calculated. Changed the regression coefficients used to convert the F11 brightness temperatures to ones from Stroeve et al. (1998). Changed parameter values from 0 to 255 (inclusive) to 0 to 245 (inclusive). Trend files are no longer being generated. Used the gsfc_25n.msk land/coast mask.
V02	Nov 2009	Removed 9-point median filter that corrected for spurious melt dates in V01 Added flags to input brightness temperatures to correct for bad scanlines, then reprocessed input brightness temperatures.
V01	Dec 2001	Original version of data.

5 RELATED DATA SETS

- MEaSUREs Arctic Sea Ice Characterization Daily 25km EASE-Grid 2.0
- DMSP SSM/I-SSMIS Daily Polar Gridded Brightness Temperatures
- Nimbus-7 SMMR Polar Radiances and Arctic and Antarctic Sea Ice Concentrations
- ESMR Polar Gridded Brightness Temperatures and Sea Ice Concentrations
- Near-Real-Time DMSP SSM/I-SSMIS Daily Polar Gridded Brightness Temperatures
- Near-Real-Time DMSP SSM/I-SSMIS Daily Polar Gridded Sea Ice Concentrations
- DMSP SSM/I-SSMIS Pathfinder Daily EASE-Grid Brightness Temperatures
- Sea Ice Concentrations from Nimbus-7 SMMR and DMSP SSM/I-SSMIS Passive Microwave Data
- Bootstrap Sea Ice Concentrations from Nimbus-7 SMMR and DMSP SSM/I
- Sea Ice Trends and Climatologies from SMMR and SSM/I-SSMIS
- NOAA/NSIDC Climate Data Record of Passive Microwave Sea Ice Concentration

6 CONTACTS AND ACKNOWLEDGMENTS

Mark Anderson
Meteorology/Climatology Program
Department of Geosciences
University of Nebraska
Lincoln, NE 68588-0340 USA

Angela C. Bliss

Oregon State University
College of Earth, Ocean and Atmospheric Sciences
104 CEOAS Admin Building
Corvallis, OR, 97331-5503 USA

Sheldon Drobot
Research Applications Lab
National Center for Atmospheric Research (NCAR)
University Corporation for Atmospheric Research (UCAR)
P.O. Box 3000
Boulder, CO 80307-3000 USA

7 REFERENCES

Abdalati, W., K. Steffen, C. Otto and K. Jezek. 1995. Comparison of brightness temperatures from SSM/I Instruments on the DMSP F8 and F11 Satellites for Antarctica and the Greenland Ice Sheet. *International Journal of Remote Sensing* 16:1223-1229.
DOI: https://doi.org/10.1080/01431169508954473

Anderson, M. 1997. Determination of a Melt Onset Date for Arctic Sea Ice Regions Using Passive Microwave Data. *Annals of Glaciology* 25:382-387.
DOI: https://doi.org/10.3189/s0260305500014324

Bliss, A. C. and M. R. Anderson. 2014. Arctic sea ice melt onset from passive microwave satellite data: 1979 - 2012. *The Crysophere* 8:2089-2100. DOI: https://doi.org/10.5194/tc-8-2089-2014

Drobot, S. and M. Anderson. 2001b. Comparison of Interannual Snowmelt Onset Dates with Atmospheric Conditions. *Annals of Glaciology* 33: 79-84.
DOI: https://doi.org/10.3189/172756401781818851

Gloersen, P. 2006. *Nimbus-7 SMMR Polar Gridded Radiances and Sea Ice Concentrations, Version 1.* [1979-1987]. Boulder, Colorado USA. NASA National Snow and Ice Data Center Distributed Active Archive Center. DOI: https://doi.org/10.5067/QOZIVYV3V9JP.

Jezek, K., C. Merry, D. Cavalieri, S., Grace, J. Bedner, D. Wilson, and D. Lampkin. 1991. Comparison Between SMMR and SSM/I Passive Microwave Data Collected over the Antarctic Ice Sheet. Byrd Polar Research Center Technical Report No. 91-03, The Ohio State University, Columbus, Ohio, 62 pp.

Maslanik, J. and J. Stroeve. 2004. *DMSP SSM/I-SSMIS Daily Polar Gridded Brightness Temperatures, Version 4.* [1988-2017]. Boulder, Colorado USA. NASA National Snow and Ice Data Center Distributed Active Archive Center. DOI: https://doi.org/10.5067/AN9AI8EO7PX0.

Meier, W. N., Khalsa, S. J. S., and M. H. Savoie. 2011. Intersensor calibration between F-13 SSM/I and F-17 SSMIs near-real-time sea ice estimates. *IEEE Trans. Geosci. Remote Sens.* 49:3343–3349. DOI: 10.1109/TGRS.2011.2117433

Meier, W., F. Fetterer, M. Savoie, S. Mallory, R. Duerr, and J. Stroeve. 2017*. NOAA/NSIDC Climate Data Record of Passive Microwave Sea Ice Concentration, Version 3.* [1979-2017]. Boulder, Colorado USA: National Snow and Ice Data Center. DOI: https://doi.org/10.7265/N59P2ZTG.

Stroeve, J., L. Xiaoming, and J. Maslanik. 1998. An Intercomparison of DMSP F11- and F13-derived Sea Ice Products. *Remote Sensing of the Environment 64:132-152.* DOI: https://doi.org/10.1175/1520-0442(2004)017<0067:DOTASI>2.0.CO;2

8 DOCUMENT INFORMATION

8.1 Publication Date

20 May 2019

8.2 Date Last Updated

30 September 2020